In vitro and Clinical Studies of Gene Therapy with Recombinant Human Adenovirus-*p53* Injection for Oral Leukoplakia

Yi Li,[1] Long-Jiang Li,[1,2] Song-Tao Zhang,[1] Li-Juan Wang,[3] Zhuang Zhang,[1] Ning Gao,[1] Yuan-Yuan Zhang,[1] and Qian-Ming Chen[1]

Abstract

Purpose: Oral leukoplakia is a well-recognized precancerous lesion of squamous cell carcinoma. When accompanied with abnormal *p53* expression, it suffered a higher risk of canceration. The present study was carried out to test whether the recombinant human adenovirus-*p53* could introduce wild-type *p53* gene to oral leukoplakia cells and induce cell cycle arrest and apoptosis.

Experimental Design: We select *p53*(-) oral dysplastic keratinocyte POE-9n, to observe the growth inhibition, cell cycle change, apoptosis-induced effects, and elaborate the corresponding molecular mechanism of recombinant adenovirus-*p53* on POE-9n cells. Meanwhile, we evaluate the feasibility, safety, and biological activity of multipoints intraepithelial injections of recombinant adenovirus-*p53* in 22 patients with dysplastic oral leukoplakia.

Results: Exogenous *p53* could be successfully transduced into POE-9n cells by recombinant adenovirus-*p53*. The optimal infecting titer in this study was multiplicity of infection (MOI) = 100. Recombinant adenovirus-*p53* could strongly inhibit cell proliferation, induce apoptosis, and arrest cell cycle in stage G_1 in POE-9n cells by inducing $p21^{CIP/WAF}$ and downregulating *bcl-2* expression. In the posttreatment patients, *p53* protein and $p21^{CIP/WAF}$ protein expression were significantly enhanced, yet *bcl-2* protein presented low expression. Sixteen patients showed clinical response to the treatment, and 14 patients showed obvious histopathologic improvement.

Conclusion: Intraepithelial injections of recombinant human adenovirus-*p53* were safe, feasible, and biologically active for patients with dysplastic oral leukoplakia. (Clin Cancer Res 2009;15(21):6724–31)

Oral leukoplakia (OLK) is defined as a white patch or plaque that cannot be clinically diagnosed as any other disease (1). Histologically, OLK is the epithelial hyperkeratosis accompanied with pure proliferation or epithelial dysplasia. It is the most common premalignant lesion of mucosa and 43% OLK develop into oral squamous cell carcinoma (2, 3), which is the sixth common malignant carcinoma in the world (4). It has been shown by previous studies (5, 6) that abnormal *p53* expression was detected in 33% to 76% of oral squamous cell carcinoma patients and 20% of OLK ones, and OLK accompanied with abnormal *p53* expression suffered a higher risk of canceration. Therefore, the effective treatment toward OLK becomes one of the preventive methods against oral squamous cell carcinoma.

The wild-type human tumor suppressor *p53* (wt-*p53*) gene is a primary mediator of cell cycle arrest, DNA repair, and apoptosis and is intimately involved in tumor development. The mutation and inactivation of *p53* is a critical event in the formation and progression of head and neck carcinoma (7, 8). Transduction of the wt-*p53* gene into OLK cells is expected to restore the tumor suppressor functions and prevent the canceration (9).

Reintroduction of wt-*p53* has been accomplished with recombinant human adenovirus-*p53* (rAd-*p53*), a replication-incompetent human type 5 adenovirus in which the E1 region has been replaced with an expression cassette containing the human wt-*p53* cDNA (10). Adenovirus delivery of the wt-*p53* gene results in strong *p53* protein expression in tumor cells with minimal toxicity to the hematopoietic system (11–15). Clinical trials results showed that rAd-*p53* is effective against a variety of malignancies, including colon, glioma, lung, ovarian, and head and neck tumors (11–17). In the clinical trials, the routes of administration typically used for rAd-*p53* were intratumoral injection (17), perfusion (18), and i.v. infusion (19).

Authors' Affiliations: [1]State Key Laboratory of Oral Diseases, [2]Department of Head and Neck Oncology, West China College of Stomatology, and [3]West China Health Hospital, Sichuan University, Chengdu, P.R. China

Received 5/21/09; revised 7/14/09; accepted 7/18/09; published OnlineFirst 10/27/09.

Grant support: National Natural Science Foundation of China: Funding number: 30471903.

The costs of publication of this article were defrayed in part by the payment of page charges. This article must therefore be hereby marked *advertisement* in accordance with 18 U.S.C. Section 1734 solely to indicate this fact.

Requests for reprints: Long-Jiang Li, State Key Laboratory of Oral Diseases, Sichuan University, Chengdu 610041, PR China; Department of Head and Neck Oncology, West China College of Stomatology, Sichuan University, Chengdu 610041, PR China. Phone: 86-28-85501440; Fax: 86-28-85582167; E-mail: muzili63@163.com and Qian-Ming Chen, State Key Laboratory of Oral Diseases, Sichuan University, Chengdu 610041, PR China. Phone and Fax: 86-28-85405251; E-mail: qmchen@scu.edu.cn.

doi:10.1158/1078-0432.CCR-09-1296

Translational Relevance

These *in vitro* and clinical studies evaluate for the first time a novel strategy to treat oral leukoplakia: gene therapy with recombinant human adenovirus-*p53* via the multipoints intraepithelial injections. The results show that exogenous *p53* can be successfully transduced and inhibit cell proliferation, induce apoptosis, and arrest cell cycle in stage G_1, and the clinical method was both safe and effective. We conclude that intraepithelial injection of recombinant adenovirus-*p53* is an effective new strategy for treating oral leukoplakia. Meanwhile, the present study provided a feasible method to block the progression of the premalignant lesions.

In this article, we selected rAd-*p53* as the intervention drug and POE-9n, an OLK cell line with negative *p53* expression, as the intervention object. Aiming to explore the molecular mechanism of rAd-*p53*, we observed changes of biological behaviors of preinfection and postinfection cells and analyzed gene expressions relating with the functional pathway of *p53*. Moreover, to evaluate the feasibility of rAd-*p53* as a clinical therapy, 22 patients with dysplastic OLK received multipoints intraepithelial injections of rAd-*p53*. The results of *in vitro* and clinical studies are reported in this article.

Materials and Methods

Cell line. POE-9n cell line was purchased from the Institute of Medical Research, Harvard University. This *p53* expression deletion cell line was derived from OLK lesion with severe epithelial dysplasia. POE-9n cells were cultured in D-keratinocyte serum–free medium supplemented with 5 ng/mL epidermal growth factor, 50 μg/mL bovine pituitary extractive (Invitrogen-Life Technologies), 100 IU/mL penicillin, and 100 μg/mL streptomycin. Cells were amplificated by using routine cell culture techniques at 37°C in 5% CO_2.

Patients. A total of 22 patients with dysplastic OLK were enrolled in the clinical trial in West China Hospital of Stomatology, Sichuan University. All the cases were confirmed by clinical and pathologic diagnosis. The average area of the lesions was 4.1 cm^2 with the largest of 7 cm^2 and the smallest of 2 cm^2. All the cases were classified as mild (nine cases), moderate (eight cases), or severe dysplasia (five cases). The patients were excluded of systemic diseases and did not receive any treatments within 3 mo. The informed consents were signed by all patients before the therapy. This study has been approved by our Institutional Review Board. The Declaration of Helsinki protocols were followed during the whole study.

Treatment protocols. rAd-*p53* (Shenzhen Sibiono Genetech Co. Ltd) was diluted by 0.9% saline solution to the concentration of 4×10^9 vp/mL before using. The whole course of treatment included 15 d, and multipoint intraepithelial injections were done on the 1st, 4th, 7th, 10th, 13th day under the local block anesthesia. With the identified best infection titer of rAd-*p53* (MOI = 100) and the reported maximum single tolerant dose (20, 21), the injection specification was determined as 2×10^9 vp/cm^2, i.e., one injection point per square centimeter and 0.5 mL rAd-*p53* solution for one point. The injection needles should be pricked into mucosa at a 30- to 45-degree angle and the depths were 2 to 3 mm according to the thickness of the lesion, to inject the solution intraepithelially. On the 15th day of the course, samples were collected for biopsy under local anesthesia. Therapeutic response of all the patients was monitored during therapeutic course and 30 d after the therapy. All patients were followed up for 24 mo and the therapeutic effects were recorded. All of the patients did not receive any therapy during the follow-up except for recurrence and cancerization.

Infection efficiency of rAd-GFP. POE-9n cells in logarithmic growth phase were seeded onto six-well plate with the concentration of 1×10^5 per well. After 24 h, rAd-GFP solution were added into the medium with the amount of MOI = 0, 25, 50, 100, 200, and 500. Cultured for another 72 h, fluorescence-activated cell sorting was done for quantitation of infection efficiency.

Cell morphology. POE-9n cells in logarithmic growth phase were seeded onto 25-mL culture flask. After 24 h of culture, rAd-*p53* of MOI = 100 was added into medium, and then the cells were cultured for another 72 h. The POE-9n infected with rAd (Shenzhen Sibiono Genetech Co. Ltd, China) of MOI = 100, which does not harbor *p53*, was set as the blank control. The cell morphology was observed under an inverted phase-contrast microscopy.

Cell growth inhibition ratio. POE-9n cells were seeded onto wells of 96-well plates at 5×10^4 cells per well and cultured for 24 h. rAd-*p53* virus solution were added into wells in the amount of MOI = 0, 25, 50, 100, 200, and 500. The control group was established with rAd of the same MOI. For each concentration, three paralleled holes were set up. Continue the cultivation for another 24, 48, 72, 96, and 120 h before the culture medium was abandoned. The proliferative activity was determined every 24 h by MTT assay at 570 nm. Growth inhibition ratio was calculated by the formula of $(OD_{control} - OD_{treated})/OD_{control} \times 100\%$.

Cell cycle and apoptosis assay. After rAd-*p53* (MOI = 100) infection for 24 and 72 h, cell cycle and apoptosis was detected by flow cytometric analysis. The POE-9n infected with rAd (MOI = 100) for 72 h was set as the control. Quantification of apoptotic cells was done by terminal deoxynucleotidyl transferase-mediated dUTP nick end labeling (TUNEL) assay using a DeadEnd Fluorometric TUNEL System (Promega, Roche). In clinical samples, similar methods were used to evaluate cell apoptosis of pre-rAd-*p53* and post-rAd-*p53*–treated patients. The correlation analysis was conducted between TUNEL staining and *p53* protein staining.

Reverse transcription-PCR and Western blotting analysis. After rAd-*p53* and rAd infection (MOI = 100) for 24 and 72 h, POE-9n cells were detected at transcript and protein level. Total RNA was extracted with TRIzol reagent (Invitrogen). First-strand cDNA was prepared from total RNA by reverse transcriptase using oligo (dT) primers, and β-actin was set as the internal control. The primers of wt-*p53*, $p21^{CIP/WAF}$, *bcl-2*, and β-actin were synthesized for PCR as following:

p53: 620 bp, upstream: 5′-TACTCCCCTGCCCTCAACAAGA-3′; downstream: 5′-CTTAGCACCTGAAGGGTGAAATATTC-3′
$p21^{CIP/WAF}$: 495 bp, upstream: 5′-TTAGGGCTTCCTCTTGGAGAAGAT-3′ downstream: 5′-ATGTCAGAACCGGCTGGGGATGTC-3′
Bcl-2: 318 bp, upstream: 5′-CGACGACTTCTCCCGCCGCTACCGC-3′ downstream: 5′-CCGCATGCTGGGGCCGTACAGTTCC-3′
β-actin: 548 bp, upstream: 5′-GTGGGGCGCCCCAGGCACCA-3′ downstream: 5′-CTCCTTAATGTCACGCACGATTC-3′

Messenger RNA expression of *p53*, $p21^{CIP/WAF}$, and *bcl-2* were investigated using reverse transcription-PCR. PCR products were separated with 1% agarose gel electrophoresis, and the results were recorded and analyzed by gel imaging system.

Cells (1×10^7) were solubilized at 4°C in lysis buffer consisting of 0.125 mol/L Tris-Cl (pH 6.8), 2% SDS, 2.5%-mercaptoethanol, and 10% glycerol. The protein levels of *p53*, $p21^{CIP/WAF}$, and *bcl-2* were detected by Western blotting, and β-actin was used as inner control.

Immunohistochemical staining. POE-9n cells were cultured for 24 h, and then rAd-*p53* and rAd (MOI = 100) were added into the medium and cultured for another 48 h. Immunohistochemical staining was carried out to detect *p53* expression according to the instruction of PV-9000 universal histostain TM-plus kits (ZYMED). The expressions of *p53*, $p21^{CIP/WAF}$, and *bcl-2* protein in samples of pre– and post–rAd-*p53* treatment were detected using the same method. The criterion of

positive expression refers to Shimizu semiquantitative grade method (22). This scoring procedure included two parts: one was based on the staining intensity, in which no, mild, moderate, and strong staining were scored as 0, 1, 2, 3; the other part was based on the rate of positive cells, in which 0 to 5%, 6 to 30%, 31 to 70%, and 71 to 100% were scored as 0, 1, 2, and 3; and the total score of 0 to 2, 3 to 4, and ≥5 were labeled as negative (-), positive (+), and strong positive (++).

Statistical analysis. Statistical analyses were done using SPSS 15.0 statistics software (SPSS). The statistical differences between two groups were evaluated by *t* test. And a χ^2/Fisher exact test was used for categorical variables. Spearman test was done to analyze the correlation of different groups. All statistical assessments were two sided and evaluated at the 0.05 level of significant difference.

Results

Infection efficiency of rAd-GFP. POE-9n cells were sensitive to adenovirus. Ten to 12 hours after rAd-GFP infection, green fluorescence could be detected under fluorescence microscope, and the fluorescence intensity reached its peak 72 hours after infection. Infection efficiencies were 36.1 ± 1.56%, 72.7 ± 1.40%, and 95.6 ± 2.76%, respectively, when MOI were 25, 50, and 100. A positive statistical correlations existed between efficiency and titer (r = 0.849; $P < 0.010$). When MOI were 200 and 500, the infection efficiencies were 97.1 ± 4.12% and 98.9 ± 1.19%, and the elevation of infection efficiency was less obvious (r = 0.124; $P > 0.05$).

Cell morphology. Under a phase-contrast microscope, POE-9n cells were observed as adherent monolayer cells, with a tight cellular alignment and polygon shapes. After infection by rAd for 72 hours, there were not significant changes of cell morphology, the cell appearance was like cobblestone with unfolding cytoplasm, and the caryocinesia was easily observed (Fig. 1A). Twenty-four hours after rAd-*p53* infection, changes of POE-9n cell morphology and growth pattern were detected. During 72 hours, POE-9n cells showed a loose arrangement, with round shrinking size, unclear outline, vacuole in the cytoplasm, karyopyknosis, partially incomplete cell membrane, and then they were departed from grouping cells and suspended in the culture solution (Fig. 1A).

Growth inhibition ratio. rAd-*p53* could significantly interfere on POE-9n cell growth. At the same time point, significantly statistical difference was determined for the OD570 values between the experimental groups ($P < 0.05$; Table 1). According to growth inhibition curve of POE-9n cell in each groups (Fig. 1B), the cell proliferative inhibition ratio gradually increased with the rAd-*p53* titer. In groups with MOI of 100, 200, and 500, the inhibition effect on POE-9n cell proliferation was significant. With the time accumulation,

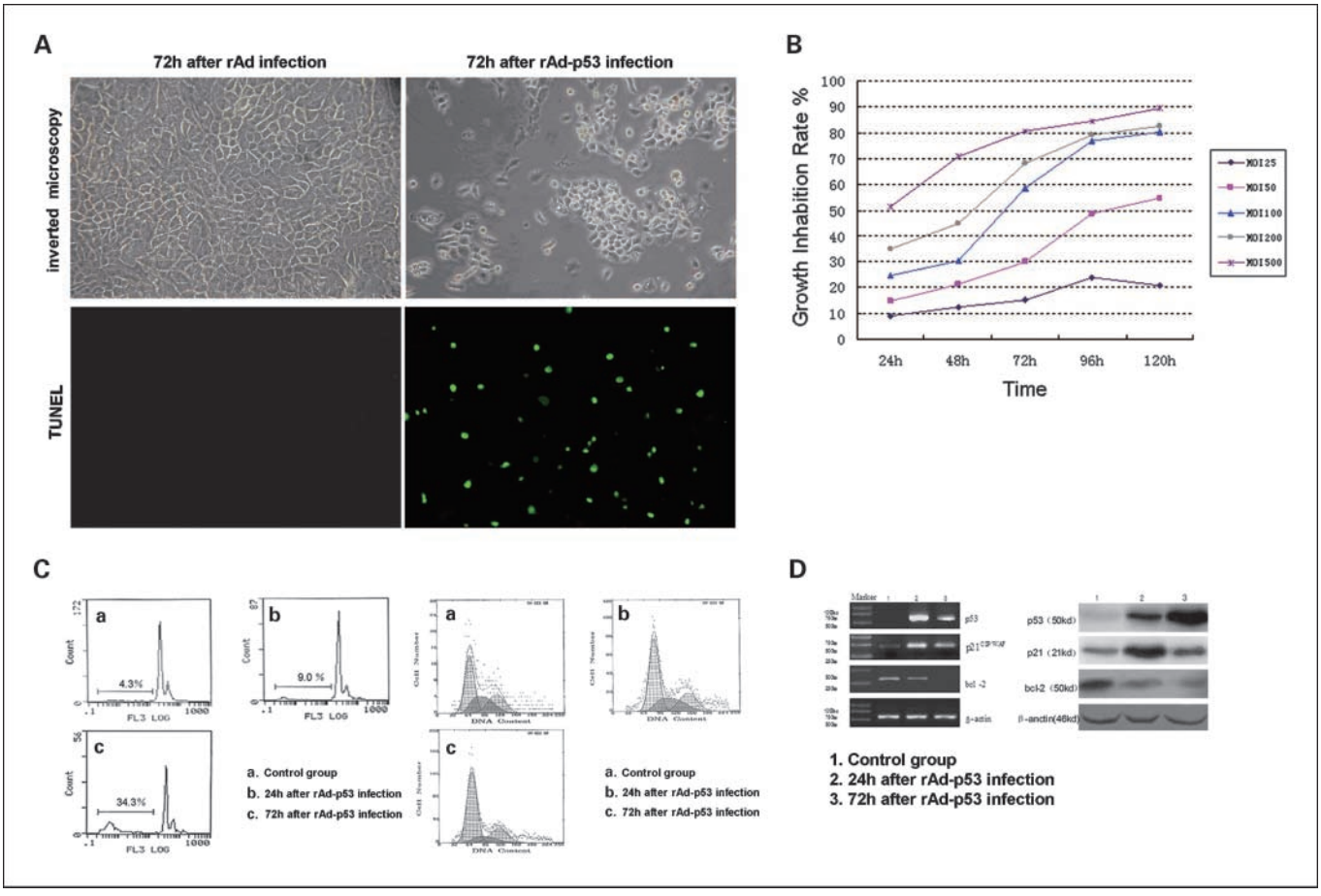

Fig. 1. Cell biology and biochemistry of POE-9n cells before and after rAd-*p53* infection. *A,* cell morphology observed with inverted microscope (×200) and TUNEL results (×100). *B,* time-activity curve of growth inhibitory of POE-9n cells induced by rAd-*p53* (MTT). *C,* flow cytometry results of POE-9n cells infected by rAd-*p53*. *Left,* cell apoptosis of POE-9n cells; *right,* cell cycle distribution of POE-9n cells. *D,* expression of mRNA by reverse transcription-PCR (*left*) and protein by West blotting (*right*) in POE-9n cells.

Table 1. Result of MTT assay (OD570 value; x ± S)

MOI	Infection time				
	24 h	48 h	72 h	96 h	120 h
0	0.9315 ± 0.0816	1.5292 ± 0.0486	1.9683 ± 0.1091	2.3458 ± 0.0756	2.6367 ± 0.0274
rAd-*p53*					
25	0.8467 ± 0.0565*	1.3347 ± 0.0165†	1.6660 ± 0.0140†	1.7828 ± 0.0262†	2.0856 ± 0.0617†
50	0.7923 ± 0.0172*	1.2020 ± 0.0249†	1.3759 ± 0.0928†	1.2013 ± 0.0476†	1.1918 ± 0.0429†
100	0.7026 ± 0.0704†	1.0669 ± 0.0503†	0.8194 ± 0.0100†	0.5442 ± 0.0640†	0.5260 ± 0.0581†
200	0.6054 ± 0.0460†	0.8456 ± 0.1240†	0.6273 ± 0.0190†	0.4914 ± 0.0346†	0.4625 ± 0.1002†
500	0.4538 ± 0.0140†	0.4499 ± 0.0125†	0.3848 ± 0.0042†	0.3688 ± 0.0190†	0.2824 ± 0.0496†
rAd					
25	0.9246 ± 0.0453	1.5185 ± 0.0562	1.9574 ± 0.0856	2.3264 ± 0.0658	2.6329 ± 0.0367
50	0.9193 ± 0.0657	1.5176 ± 0.0387	1.9452 ± 0.0695	2.3178 ± 0.0679	2.62867 ± 0.0569
100	0.9125 ± 0.0328	1.5059 ± 0.0795	1.9446 ± 0.0359	2.3076 ± 0.0756	2.6255 ± 0.0965
200	0.9018 ± 0.0475	1.4961 ± 0.0154	1.9227 ± 0.0759	2.2953 ± 0.0382	2.5067 ± 0.0859
500	0.8561 ± 0.0613*	1.4124 ± 0.1016*	1.8253 ± 0.0465*	1.9853 ± 0.0276†	2.2564 ± 0.0517†

*$P < 0.05$ compared with the control group.
†$P < 0.01$ compared with the control group.

the increase of inhibition effect in these three groups slowed down gradually ($P > 0.05$). At the time points of 96 and 120 hours, no significant difference in the inhibition effect was detected among the three groups with MOI of 100, 200, and 500. The maximum inhibition efficiency of rAd-*p53* on POE-9n cell growth was ~80%. In the control groups, when MOI of rAd was in the range of 100 to 500, no significant difference was detected in proliferative inhibition ratio of POE-9n cell, whereas in the MOI = 500 group, significant cytotoxic effect was observed (Table 1). The above results indicated that rAd-*p53* exerted inhibition effect on POE-9n cell growth, and MOI = 100 could be determined as the ideal titer for POE-9n cell rAd-*p53* infection, which was able to maintain a relatively high infection efficiency as well as to avoid interference by the cell toxic action of the adenovirus.

Apoptosis and cell cycle. The apoptosis of POE-9n cells after rAd-*p53* infection was detected with flow cytometry and TUNEL method. Results of flow cytometry showed (Fig. 1C) the following: no significant subdiploid apoptotic peak was observed in the control group (3.8 ± 1.46%); 24 hours after rAd-*p53* infection, the cell apoptosis percentage was increased, but with a relatively small increasing amplitude (9.0 ± 0.87%); 72 hours after rAd-*p53* infection, significant apoptotic peak was observed (34.3 ± 2.01%). Meanwhile, TUNEL results showed (Fig. 1A) the following: almost no apoptotic cell in the control group was observed under microscope (1.3 ± 0.15%); 24 hours after rAd-*p53* infection, only a few cell apoptosis was observed (16.9 ± 2.39%); apoptosis was observed for most of the cells under microscope 72 hours after rAd-*p53* infection (65.3 ± 3.01%). There was a significant statistical difference when the 72-h group was compared with the control and 24-h groups ($P < 0.01$). Consistent results of flow cytometry and TUNEL were obtained with statistical analysis. In case samples, positive TUNEL staining was mainly located in the nucleus, with the appearance of densely arranged prunosus grains. No positive staining of individual cells was observed in the pretreatment samples of 22 cases. In posttreatment samples, abundant typical cell apoptosis was detected in 18 cases (81.8%; Table 2), especially in tissues with strong positive *p53* expression ($P < 0.01$). But the TUNEL staining strap was not that of *p53* staining, and no *p53*-positive staining was detected in TUNEL staining cells.

The distribution change of cell cycle of posttransduction POE-9n cells was analyzed with flow cytometry (Fig. 1C). In the control group, percentages of stage G_1, S, and G_2 were 42.3 ± 2.52%, 31.2 ± 1.56%, and 26.5 ± 1.53%, respectively. Twenty-four and 72 hours after rAd-*p53* infection, the percentages of stage G_1, S, and G_2 were 51.7 ± 1.47% and 64.0 ± 3.91%, 25.5 ± 4.10% and 12.9 ± 2.46%, and 22.8 ± 0.49% and 23.1 ± 1.83%, respectively. There were significant statistical differences in the comparison among the three groups ($P < 0.01$). It was shown that after rAd-*p53* infection, POE-9n cell percentage of stage G_1 increased significantly, percentage of stage S decreased significantly, and percentage of stage G_2 showed no significant change.

Messenger RNA and protein expression of p53, p21$^{CIP/WAF}$, and bcl-2. Messenger RNA and protein expressions of *p53*, *p21$^{CIP/WAF}$*, and *bcl-2* in POE-9n cells were examined by semiquantitative reverse transcription-PCR and Western blotting, respectively (Fig. 1D). Consistent results were obtained with those two methods. In the control group, no change was detected for mRNA and protein expression of *p53*, whereas in rAd-*p53* group, high expression of *p53* mRNA and protein was observed 24 hours after the transduction, and during 72 hours after transduction, *p53* mRNA expression was reduced and *p53* protein expression maintained a continuous increase. *P21$^{CIP/WAF}$* mRNA and protein experienced a significant increase after rAd-*p53* infection compared with the control group, whereas *bcl-2* mRNA and protein experienced a significant decrease 72 hours after transduction (Fig. 1D).

Immunohistochemical staining. Almost all POE-9n cells infected by rAd-*p53* displayed strong positive expression of *p53* protein. The positive products were located in the nucleus and some of the kytoplasm, with the appearance of dark brown grains. However, in the control group, no *p53* protein expression was observed (Fig. 2A).

According to the comparison of pretreatment and posttreatment pathologic samples, the H&E staining of post–rAd-*p53* injection tissues displayed thinning of the cuticular layer, tight

cellular arrangement, decrease or elimination of atypical cells (14 of 22, 63.6%), and mild to severe inflammatory cell infiltration in the proper layer (16 of 22, 72.7%; Fig. 2B). Results of immunohistochemical staining were shown in Table 2. Positive staining of *p53* protein was mainly located in the nucleus, with the appearance of densely arranged dark yellow grains. In samples of pretreatment cases, 10 cases displayed negative expression (45.5%), 12 cases displayed low-level expression (55.5%), and the cells with positive expression were dispersed in different layers of epithelium (Fig. 2B). In samples of posttreatment cases, positive *p53* protein expression was observed in all 22 cases (100%), and the positive staining was mainly located in the basal and spinous layer of epithelium, forming a significant dark yellow staining strap (Fig. 2B). No correlation was determined between the *p53* statuses of pretreatment and posttreatment tissues ($P > 0.05$).

Positive $p21^{CIP/WAF}$ protein staining was mainly located in the nucleus and cytoplasm, with the appearance of densely arranged dark yellow grains. In pretreatment tissues, only five cases displayed positive expression (22.7%), which was different from that of *p53* protein staining, and the cells with positive expression were dispersed in different layers of epithelium (Fig. 2C). In posttreatment samples, 19 cases displayed high expression of $p21^{CIP/WAF}$ protein (86.4%), which was similar to that of *p53* protein staining, and $p21^{CIP/WAF}$ protein was mainly located in the basal and spinous layer of epithelium (Fig. 2C). According to statistical analysis, $p21^{CIP/WAF}$ expression was significant increased in posttreatment tissues ($P < 0.01$), sharing positive correlation with the expression of *p53* protein ($P < 0.01$).

Positive *bcl-2* protein staining was mainly located in the kytoplasm, with the appearance of a densely arranged dark yellow grain ring. In pretreatment tissues, 12 cases displayed mild to strong positive expression (54.5%), which was different from that of $p21^{CIP/WAF}$ protein (Fig. 2D); in posttreatment tissues, only 4 cases displayed positive expression (18.2%), in which only a few positive basal cells and adjacent inflammatory cells were observed (Fig. 2D). It was shown by statistical analysis that *bcl-2* expression was significantly decreased after local rAd-*p53* injection ($P < 0.01$), sharing negative correlation with the expression of *p53* protein ($P < 0.01$).

The initial clinical effect of rAd-p53. All of 22 patients with OLK completed the treatment course on schedule. Eighteen patients (81.8%) displayed mucous membrane necrosis of different degree in the lesion regions after rAd-p53 treatment. After 24 months of follow-up, 5 cases experienced a complete regression of the disease (22.7%), 20% to 70% areas of the lesion disappeared in 11 cases (50%), 4 cases did not receive significant therapeutic effect (18.2%), and 2 cases were diagnosed as focal cancerization and received an extensive resection (9.1%). No severe dose-restriction toxicity and side effects was observed in all of the patients. The most common side effect was transient fever, which was encountered in 7 patients (31.8%) and generally emerged in 2 to 12 hours after first or secondary rAd-*p53* injection, with the highest temperature of 38.9°C and duration of 3 to 5 hours. Besides, five patients (22.7%) complained about pain in the injection point, two patients (9.1%) experienced flu-like symptoms after the first injection, and four patients (18.2%) had a transient increase of WBC count in hematologic test after the therapy.

Discussion

Since the initial report on *p53* gene in 1979 (23), the structural change and abnormal expression of *p53* gene has been shown as a key procedure for tumor genesis and development (24). Wild-type *p53* gene possesses a function of inhibiting carcinogenesis by maintaining genomic integrity. Therefore, *p53* gene is also called as "housekeeping gene" (25). When *p53* gene deletion or mutation occurs, cells could not enter into stage G_1 and DNA reparation via *p53*-mediated pathway after DNA injury; therefore, cells with injured genetic information could enter into proliferation and finally induce malignant tumor (26, 27). rAd-*p53* shared a high sensitivity toward tumor cells, and by intratumor injection, wild-type *p53* could be successfully transduced and perform multiple antitumor actions (14, 27, 28). Introduction of rAd-*p53* into eight different types of carcinoma of head and neck could induce significant cell growth inhibition in 14.5% to 47% cells (29). It has been shown by many preclinical trials that rAd-*p53* treatment could induce cell apoptosis of different degrees in various kinds of malignant tumor cells (30–32), and this effect was not associated with *p53* gene condition of the tumor cells (32).

Various cells have different sensitivities to adenovirus (33, 34), and the adenovirus cytotoxicity has significant relationships with the titer and infection time (35). The cytotoxicity was significant when MOI reached above 500, and there was no influence on cell growth when MOI was below 50 (36–38). In present research, relatively stable infecting efficiency (>95%) could be obtained when MOI of rAd was in the range of 100 to 500, and no significant difference was detected in proliferative inhibition ratio of POE-9n cell in MTT experiment, whereas in the MOI = 500 group, significant cytotoxic effect was observed. A significant positive staining of *p53* protein in nucleus or kytoplasm was observed in almost all cells after rAd-*p53* infection by the titer of MOI = 100, indicating that when MOI was 100, rAd-*p53* infection could effectively

Table 2. Biological analysis in biopsy specimens

Result	Specimens before treatment				Specimens after treatment			
	p53	*p21*	*bcl-2*	TUNEL	*p53*	*p21*	*bcl-2*	TUNEL
-	10	17	10	22	0	3	18	4
+	12	5	6	0	5	11	4	10
++	0	0	6	0	17	8	0	8
Positive rate	54.5%	22.7%	54.5%	0%	100%	86.4%	18.2%	81.8%

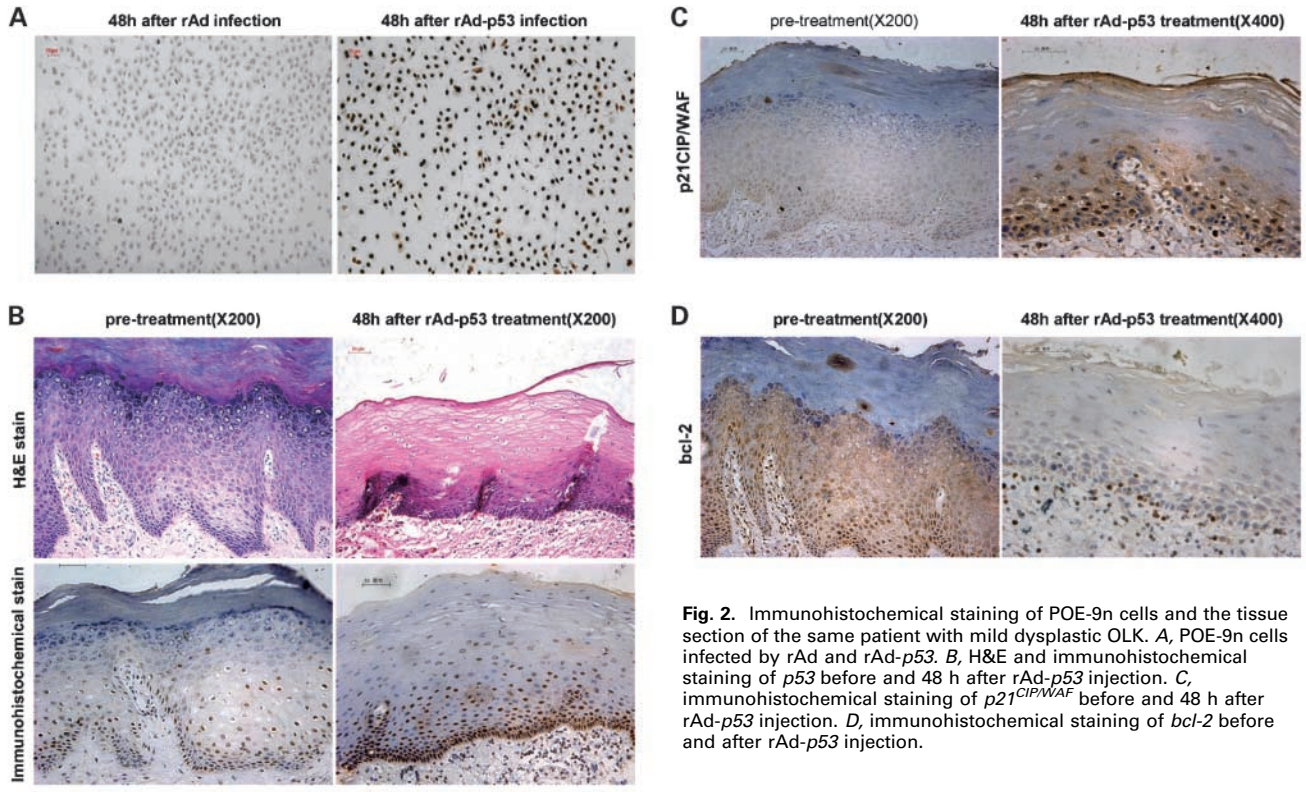

Fig. 2. Immunohistochemical staining of POE-9n cells and the tissue section of the same patient with mild dysplastic OLK. *A*, POE-9n cells infected by rAd and rAd-*p53*. *B*, H&E and immunohistochemical staining of *p53* before and 48 h after rAd-*p53* injection. *C*, immunohistochemical staining of $p21^{CIP/WAF}$ before and 48 h after rAd-*p53* injection. *D*, immunohistochemical staining of *bcl-2* before and after rAd-*p53* injection.

introduce exogenous *p53* gene into POE-9n cells, and decrease the toxicity and side effects of adenovirus as far as possible.

Cell morphologic change is one of the basic indexes for cell activity. Change of POE-9n cell morphology and growth characteristic was observed 24 hours after rAd-*p53* infection, and typical morphologic change was detected 72 hours after rAd-*p53* infection. These indicated that rAd-*p53* could inhibit POE-9n cell proliferation by interfering with cell metabolism and changing the character of cell envelope. We also examined the apoptosis of POE-9n cells after rAd-*p53* infection with flow cytometry and TUNEL, and similar results were obtained with the two methods. It was discovered that the apoptosis percentage of rAd-*p53*–treated groups was all higher than that of the control group, especially 72 hours after transduction, which indicated that rAd-*p53* could induce apoptosis of oral hyperplastic cells and had a good application perspective for the inhibition of OLK malignant transformation.

Cell cycle plays an important role in cell proliferation, differentiation, and tumor progression, which is regulated by intracellular and extracellular signal transduction pathway as well as feedback loop (39). The G_1-S checkpoint is the key point in the regulation of cell proliferation (40, 41). One of the significant activities of wild-type *p53* gene is to regulate G_1-S checkpoint by coding normal *p53* protein to stagnate cells with DNA damage at stage G_1 for DNA reparation. It was discovered by Von Gruenigen et al. (42) that introduction of Ad-CMV-*p53* (MOI = 100) into ovarian cancer cells (OVCAR-3) could stagnate all cells at stage G_1 (100%). According to the study of Wu et al. (43) on ovarian cancer cells (2774qw), significant accumulation of stage G_1 cells was observed 4 hours after rAd-*p53* infection, significant decrease of stage S cells was encountered 20 hours after infection, and stage G_2 cells experienced no significant change. Similar to the above researches, in the present study, it was discovered that cells of stage G_1 significantly increased, cells of stage S significantly decreased, and cells of stage G_2 experienced no change in rAd-*p53*–treated POE-9n cells 24 hours after infection, and abundant cell apoptosis was observed 72 hours after infection, all of which indicated that rAd-*p53* could successfully introduce exogenous *p53* into POE-9n cells and induce stage G_1 stagnation.

Based on the study of rAd-*p53* influence on apoptosis and cell cycle of POE-9n cell, the expression of the key molecule of *p53* passage ($p21^{CIP/WAF}$, *bcl-2*) was further detected, in an attempt to explore the associated molecular mechanism of rAd-*p53* on POE-9n cells. $p21^{CIP/WAF}$ gene is the first cyclin-dependent kinase–inhibiting factor discovered in mammalian recently (44), which could bind with almost all cyclin-dependent kinase compound, and induce stage G_1 stagnation (45). As the main downstream molecule of *p53* gene in cell cycle regulation, the binding site of wild-type *p53* gene has been detected at upstream 2.4 Kbm of $p21^{CIP/WAF}$ gene, and *p53* could upregulate $p21^{CIP/WAF}$ expression at transcriptional level, whereas mutant *p53* has not such function (46). In this study, the POE-9n cells were *p53* gene deletion cells, and $p21^{CIP/WAF}$ was unactivated; therefore, the basic mRNA level was quite low. After introduction of exogenous *p53* into POE-9n cells by rAd-*p53*, mRNA and protein expression of $p21^{CIP/WAF}$ was significantly elevated, which was positively correlated with *p53* protein by the statistical analysis, indicating that rAd-*p53* could upregulate $p21^{CIP/WAF}$ expression to regulate cell cycle.

Exogenous passage of *p53*-dependent cell apoptosis network is usually activated during DNA damage, which is regulated by *bcl-2* family (47). *p53* gene could precisely regulate cell apoptosis via activating the apoptosis promoter of *bcl-2* family such as bax, BH3, and bid, or inhibiting the antiapoptosis molecules such as *bcl-2*, bcl-xl, and survivin. It was discovered in this study that relatively high expression of *bcl-2* mRNA and protein existed in normal POE-9n cells, which significantly decreased 72 hours after rAd-*p53* infection. The statistical analysis showed the negative correlation between protein expressions of *bcl-2* and *p53*, indicating that exogenous *p53* inhibited *bcl-2* expression and induced the apoptosis.

The biological reaction of rAd-*p53* treatment in OLK was observed by immunohistochemical staining of exogenous *p53* protein and its function proteins like $p21^{CIP/WAF}$ and *bcl-2*, as well as TUNEL staining of apoptotic cells. High *p53* protein expression was observed in tissues after local rAd-*p53* injection. The positive staining was mainly located in basal and spinous layer of epithelium and formed a significant dark yellow staining strap, which was significantly different from the dispersed arrangement of *p53* protein in pretreated tissues. Meanwhile, the primary *p53*-negative staining tissue displayed high *p53* expression after rAd-*p53* therapy with no exception, further indicating the successful transduction of exogenous *p53* gene, which also confirmed that exogenous *p53* gene transduction was not associated with the primary *p53* gene condition of the disease (36). And we deemed that the clinical responses were only correlated with the rAd-p53 transduction, but not with the primary *p53* status. Therefore, it was speculated that after successful transduction, *p53* gene exerted the action of transcription factor via activating $p21^{CIP/WAF}$ and inhibiting *bcl-2*, and therefore performed the activities of influencing cell cycle, inducing cell apoptosis and inhibiting cell growth of abnormal hyperplasia.

Besides, the biological function of exogenous *p53* was shown by TUNEL staining. Typical TUNEL staining of apoptotic cell was detected in 83.3% rAd-*p53* posttreatment tissues, and a significant correlation was determined between TUNEL and *p53* staining. However, we discovered that TUNEL staining strap was located in the upper layer of epithelial tissue, not as the *p53* staining strap, which was in the basal layer and spinous layer. This phenomenon might be associated with the time effect of *p53*-inducing cell apoptosis (12). Namely, cells of the upper layer were first infected by rAd-*p53*, which induced *in situ* apoptosis with clinical manifestation of surface layer necrosis of mucous membrane.

Although the involved case number and follow-up time was rather limited in this study, we observed the therapeutic effect of rAd-*p53* injection in OLK after 24 months. Significant clinical effect was detected in 16 patients, and meanwhile, 63.6% patients displayed pathologic improvement. Compared with traditional therapy (21), the result was exciting. The common side effects after rAd-*p53* injection included transient fever, flu-like symptoms, and transient increase of WBC number, which were the inflammatory reaction of the patients toward viral vector. We also observed a large amount of local inflammatory cell infiltration in H&E sections of the posttreatment tissues. Compared with other clinical reports (14, 28), the toxic and side effects induced by rAd-*p53* injection in this study was slighter, which might be owed to the relatively low dose as a result of the special lamellar lesion of OLK. However, we have to admit that as a result of the limited case number and follow-up time in this study, the evaluation of therapeutic effects of intraepithelial rAd-*p53* injection in the treatment of OLK requires further expansion of the sample size and extension of the follow-up period for confirmation.

In conclusion, with short term clinical research of this study, it was shown that rAd-*p53* could successfully introduce exogenous wild-type *p53* gene into the cells of OLK and exert biological effects. Multipoint intraepithelial rAd-*p53* injection in the treatment of hyperplastic OLK was safe and feasible. The results of this research provided a new way for the further clinical application.

Disclosure of Potential Conflicts of Interest

No potential conflicts of interest were disclosed.

References

1. Axell T, Pindborg JJ, Smith CJ, van der Waal I. Oral white lesions with special reference to precancerous and tobacco-related lesions: conclusions of an international symposium held in Uppsala, Sweden, May 18-21 1994. International Collaborative Group on Oral White Lesions. J Oral Pathol Med 1996;25:49–54.
2. Liu SC, Klein-Szanto AJ. Markers of proliferation in normal and leukoplakic oral epithelia. Oral Oncol 2000;36:145–51.
3. Reibel J. Prognosis of oral pre-malignant lesions: significance of clinical, histopathological, and molecular biological characteristics. Crit Rev Oral Biol Med 2003;14:47–62.
4. Parkin DM, Bray F, Ferlay J, Pisani P. Estimating the world cancer burden: Globocan 2000. Int J Cancer 2001;94:153–6.
5. Gleich LL, Salamone FN. Molecular genetics of head and neck cancer. Cancer Control 2002;9: 369–78.
6. Vora HH, Trivedi TI, Shukla SN, Shah NG, Goswami JV, Shah PM. p53 expression in leukoplakia and carcinoma of the tongue. Int J Biol Markers 2006;21:74–80.
7. Ries JC, Schreiner D, Steininger H, Girod SC. p53 mutation and detection of p53 protein expression in oral leukoplakia and oral squamous cell carcinoma. Anticancer Res 1998;18: 2031–6.
8. Sakai E, Tsuchida N. Most human squamous cell carcinomas in the oral cavity contain mutated p53 tumor-suppressor genes. Oncogene 1992; 7:927–33.
9. Tetu B, Brisson J, Plante V, Bernard P. p53 and c-erbB-2 as markers of resistance to adjuvant chemotherapy in breast cancer. Mod Pathol 1998;11: 823–30.
10. Brand K, Klocke R, Possling A, Paul D, Strauss M. Induction of apoptosis and G_2/M arrest by infection with replication-deficient adenovirus at high multiplicity of infection. Gene Ther 1999;6: 1054–63.
11. Buller RE, Runnebaum IB, Karlan BY, et al. A phase I/II trial of rAd/p53 (SCH 58500) gene replacement in recurrent ovarian cancer. Cancer Gene Ther 2002;9:553–66.
12. Lang FF, Bruner JM, Fuller GN, et al. Phase I trial of adenovirus-mediated p53 gene therapy for recurrent glioma: biological and clinical results. J Clin Oncol 2003;21:2508–18.
13. Modesitt SC, Ramirez P, Zu Z, Bodurka-Bevers D, Gershenson D, Wolf JK. *In vitro* and *in vivo* adenovirus-mediated p53 and p16 tumor suppressor therapy in ovarian cancer. Clin Cancer Res 2001;7:1765–72.
14. Schuler M, Herrmann R, De Greve JL, et al. Adenovirus-mediated wild-type p53 gene transfer in patients receiving chemotherapy for advanced non-small-cell lung cancer: results of a multicenter phase II study. J Clin Oncol 2001; 19:1750–8.
15. Spitz FR, Nguyen D, Skibber JM, Meyn RE, Cristiano RJ, Roth JA. Adenoviral-mediated wild-type p53 gene expression sensitizes colorectal cancer cells to ionizing radiation. Clin Cancer Res 1996;2:1665–71.
16. Pan JJ, Zhang SW, Chen CB, et al. Effect of recombinant adenovirus-p53 combined with radiotherapy on long-term prognosis of advanced nasopharyngeal carcinoma. J Clin Oncol 2009; 27:799–804.
17. Weill D, Mack M, Roth J, et al. Adenoviral-mediated p53 gene transfer to non-small cell lung cancer through endobronchial injection. Chest 2000;118:966–70.
18. Pagliaro LC, Keyhani A, Williams D, et al. Repeated intravesical instillations of an adenoviral vector in patients with locally advanced bladder

cancer: a phase I study of p53 gene therapy. J Clin Oncol 2003;21:2247–53.
19. Reid T, Warren R, Kirn D. Intravascular adenoviral agents in cancer patients: lessons from clinical trials. Cancer Gene Ther 2002;9:979–86.
20. Sankaranarayanan R, Mathew B, Varghese C, et al. Chemoprevention of oral leukoplakia with vitamin A and β carotene: an assessment. Oral Oncol 1997;33:231–6.
21. Scardina GA, Carini F, Maresi E, Valenza V, Messina P. Evaluation of the clinical and histological effectiveness of isotretinoin in the therapy of oral leukoplakia: ten years of experience: is management still up to date and effective? Methods Find Exp Clin Pharmacol 2006;28:115–9.
22. Shimizu M, Saitoh Y, Itoh H. Immunohistochemical staining of Ha-ras oncogene product in normal, benign, and malignant human pancreatic tissues. Hum Pathol 1990;21:607–12.
23. Linzer DI, Levine AJ. Characterization of a 54 K dalton cellular SV40 tumor antigen present in SV40-transformed cells and uninfected embryonal carcinoma cells. Cell 1979;17:43–52.
24. Hollstein M, Sidransky D, Vogelstein B, Harris CC. p53 mutations in human cancers. Science 1991;253:49–53.
25. Levine AJ. p53, the cellular gatekeeper for growth and division. Cell 1997;88:323–31.
26. Balint EE, Vousden KH. Activation and activities of the p53 tumour suppressor protein. Br J Cancer 2001;85:1813–23.
27. Harris CC. Structure and function of the p53 tumor suppressor gene: clues for rational cancer therapeutic strategies. J Natl Cancer Inst 1996; 88:1442–55.
28. Pisters LL, Pettaway CA, Troncoso P, et al. Evidence that transfer of functional p53 protein results in increased apoptosis in prostate cancer. Clin Cancer Res 2004;10:2587–93.
29. Higuchi Y, Asaumi J, Murakami J, et al. Effects of p53 gene therapy in radiotherapy or thermotherapy of human head and neck squamous cell carcinoma cell lines. Oncol Rep 2003;10:671–7.
30. Huang Y, Jin Y, Yan CH, et al. Involvement of Annexin A2 in p53 induced apoptosis in lung cancer. Mol Cell Biochem 2008;309:117–23.
31. Kornberg L. Ad-fRNK and Ad-p53 cooperate to augment drug-induced death of a transformed cell line. Anticancer Res 2006;26:3025–31.
32. Quist SR, Wang-Gohrke S, Kohler T, Kreienberg R, Runnebaum IB. Cooperative effect of adenoviral p53 gene therapy and standard chemotherapy in ovarian cancer cells independent of the endogenous p53 status. Cancer Gene Ther 2004;11:547–54.
33. Romano G, Michell P, Pacilio C, Giordano A. Latest developments in gene transfer technology: achievements, perspectives, and controversies over therapeutic applications. Stem Cells 2000;18:19–39.
34. Walters RW, Grunst T, Bergelson JM, Finberg RW, Welsh MJ, Zabner J. Basolateral localization of fiber receptors limits adenovirus infection from the apical surface of airway epithelia. J Biol Chem 1999;274:10219–26.
35. Frey BM, Hackett NR, Bergelson JM, et al. High-efficiency gene transfer into *ex vivo* expanded human hematopoietic progenitors and precursor cells by adenovirus vectors. Blood 1998;91:2781–92.
36. Johnson KT, Rodicker F, Heise K, et al. Adenoviral p53 gene transfer inhibits human Tenon's capsule fibroblast proliferation. Br J Ophthalmol 2005;89:508–12.
37. Lou J, Xu F, Merkel K, Manske P. Gene therapy: adenovirus-mediated human bone morphogenetic protein-2 gene transfer induces mesenchymal progenitor cell proliferation and differentiation *in vitro* and bone formation *in vivo*. J Orthop Res 1999;17:43–50.
38. Watanabe T, Kuszynski C, Ino K, et al. Gene transfer into human bone marrow hematopoietic cells mediated by adenovirus vectors. Blood 1996;87:5032–9.
39. Peter M, Herskowitz I. Joining the complex: cyclin-dependent kinase inhibitory proteins and the cell cycle. Cell 1994;79:181–4.
40. Rieder CL, Cole RW, Khodjakov A, Sluder G. The checkpoint delaying anaphase in response to chromosome monoorientation is mediated by an inhibitory signal produced by unattached kinetochores. J Cell Biol 1995;130:941–8.
41. Bartek J, Lukas J. Mammalian G1- and S-phase checkpoints in response to DNA damage. Curr Opin Cell Biol 2001;13:738–47.
42. Von Gruenigen VE, O'Boyle JD, Coleman RL, Wilson D, Miller DS, Mathis JM. Efficacy of intraperitoneal adenovirus-mediated p53 gene therapy in ovarian cancer. Int J Gynecol Cancer 1999; 9:365–72.
43. Wu Q, Kirschmeier P, Hockenberry T, et al. Transcriptional regulation during p21WAF1/CIP1-induced apoptosis in human ovarian cancer cells. J Biol Chem 2002;277:36329–37.
44. Stewart ZA, Pietenpol JA. p53 Signaling and cell cycle checkpoints. Chem Res Toxicol 2001;14:243–63.
45. Harper JW, Adami GR, Wei N, Keyomarsi K, Elledge SJ. The p21 Cdk-interacting protein Cip1 is a potent inhibitor of G1 cyclin-dependent kinases. Cell 1993;75:805–16.
46. Waldman T, Kinzler KW, Vogelstein B. p21 is necessary for the p53-mediated G1 arrest in human cancer cells. Cancer Res 1995;55: 5187–90.
47. Haupt S, Berger M, Goldberg Z, Haupt Y. Apoptosis—the p53 network. J Cell Sci 2003; 116:4077–85.